Published in final edited form as:
Dev Biol. 2011 May 15; 353(2): 266–274. doi:10.1016/j.ydbio.2011.02.029.

Hox genes define distinct progenitor sub-domains within the second heart field

Nicolas Bertrand[1,§,*], **Marine Roux**[1,§], **Lucile Ryckebüsch**[1,+], **Karen Niederreither**[2], **Pascal Dollé**[3], **Anne Moon**[4], **Mario Capecchi**[5], and **Stéphane Zaffran**[1,*]

[1] Laboratoire de Génétique Médicale et Génomique Fonctionnelle, Inserm UMR_S910, Université d'Aix-Marseille, 27 Bd Jean Moulin, 13005 Marseille, France

[2] Department of Nutritional Sciences, Dell Pediatric Research Institute, University of Texas, Austin, TX, USA

[3] Institut de Génétique et de Biologie Moléculaire et Cellulaire (IGBMC), Inserm U964/Centre National de Recherche Scientifique (CNRS) UMR 1704/Université de Strasbourg, 67404 Illkirch, France

[4] Program in Molecular Medicine, Departments of Pediatrics, Neurobiology and Anatomy, and Human Genetics, University of Utah, Salt Lake City, UT, USA

[5] Howard Hughes Medical Institute, University of Utah, Salt Lake City, UT, USA

Abstract

Much of the heart, including the atria, right ventricle and outflow tract (OFT) is derived from a progenitor cell population termed the second heart field (SHF) that contributes progressively to the embryonic heart during cardiac looping. Several studies have revealed anterior-posterior patterning of the SHF, since the anterior region (anterior heart field) contributes to right ventricular and OFT myocardium whereas the posterior region gives rise to the atria. We have previously shown that Retinoic Acid (RA) signal participates to this patterning. We now show that *Hoxb1*, *Hoxa1*, and *Hoxa3*, as downstream RA targets, are expressed in distinct sub-domains within the SHF. Our genetic lineage tracing analysis revealed that *Hoxb1*, *Hoxa1* and *Hoxa3*-expressing cardiac progenitor cells contribute to both atria and the inferior wall of the OFT, which subsequently gives rise to myocardium at the base of pulmonary trunk. By contrast to *Hoxb1*^{Cre}, the contribution of *Hoxa1-enhIII-Cre* and *Hoxa3*^{Cre}-labeled cells is restricted to the distal regions of the OFT suggesting that proximo-distal patterning of the OFT is related to SHF sub-domains characterized by combinatorial *Hox* genes expression. Manipulation of RA signaling pathways showed that RA is required for the correct deployment of *Hox*-expressing SHF cells. This report provides new insights into the regulatory gene network in SHF cells contributing to the atria and sub-pulmonary myocardium.

[*]Corresponding authors: Stéphane Zaffran or Nicolas Bertrand, Inserm UMR_S910, Université d'Aix-Marseille, Faculté de Médecine, 27 Bd Jean Moulin, 13005 Marseille, France, Phone: +33 4 91 32 43 86, Fax: +33 4 91 79 72 27, stephane.zaffran@univmed.fr or nicolas.bertrand@univmed.fr.
[§]These authors contributed equally to this work
[+]Present address: Division of Biological Sciences, University of California, San Diego, 9500 Gilman Dr., La Jolla, ca 92093-0347

Keywords

Retinoic Acid; Heart development; Mouse; Hox genes; Cardiac progenitor cells

INTRODUCTION

The four-chambered mammalian heart forms from a heterogeneous population of progenitor cells in anterior lateral mesoderm. Studies in mouse and chick have established that the heart forms from two sources of progenitor cells (Buckingham et al., 2005; Vincent and Buckingham, 2010). As the embryo grows, cells of the cardiac crescent fuse at the midline to form the primitive heart tube. The primitive heart tube initially functions to support the embryonic circulation and provides a scaffold into which the cells from the second heart field (SHF) migrate prior to chamber morphogenesis. SHF cells are first located medially to the cardiac crescent, and subsequently reside in mesoderm underlying the pharynx before they accrue to the heart. The contribution of this population of cardiac progenitors to the heart was revealed by studies of the LIM transcription factor *Islet1* (*Isl1*), which is a pan-marker of the SHF (Cai et al., 2003). The rostral part of the SHF, the anterior heart field (AHF), which is marked by *Fgf10* expression (Kelly et al., 2001) contributes to the formation of right ventricular and outflow tract (OFT) myocardium (Zaffran et al., 2004), whereas cells in the posterior SHF (Cai et al., 2003) expressing *Isl1*, but not AHF markers, contribute to atrial myocardium (Galli et al., 2008). These data indicate that the SHF is patterned along the anterior-posterior (AP) axis of the mouse embryo, however, a detailed understanding of the molecular regulatory pathways governing this process is lacking.

We have recently shown that the retinoic acid (RA) signaling pathway plays a potent role in limiting cardiac specification. Mouse embryos lacking the RA synthesis enzyme Raldh2 have an expanded SHF, resulting in morphogenetic defects at both the arterial and venous poles (Ryckebusch et al., 2008). Consistent with this, zebrafish embryos lacking RA signaling exhibit an excess of cardiac progenitor cells in the lateral mesoderm (Keegan et al., 2005). In the avian model, RA signaling promotes atrial cell identity within the heart field (Xavier-Neto et al., 1999; Xavier-Neto et al., 2001; Hochgreb et al., 2003). It remains unknown whether the functions of RA signaling on SHF development and cardiac identity are distinct or overlapping. Identifying RA-target genes in cardiac progenitor cells will help to elucidate the mechanisms downstream of RA signaling that delimit the SHF. Studies in zebrafish embryos demonstrated that *Hoxb5b*, expressed in the forelimb field, acts downstream of RA signaling to restrict the number of cardiac progenitor cells (Waxman and Yelon, 2009). Thus, we hypothesized that some of the homeobox (*Hox*) genes may be functional targets of RA in cardiac lineages in the mouse.

Hox genes are a large family of related genes that encode homeodomain transcription factors. Mammalian *Hox* genes are clustered in four chromosomal loci (the Hox clusters), and play an important role in regulating the specification of positional identities along the AP axis during development (Alexander et al., 2009; Wellik, 2009). Within each cluster, the genes are arranged in a sequence that reflects their sequential activation during development (temporal collinearity) (Izpisua-Belmonte et al., 1990) and the position of the anterior boundary of their expression domains along the AP body axis (spatial collinearity) (Duboule and Dolle, 1989; Graham et al., 1989). Initial *Hox* transcription and rostral expansion of *Hox* expression domains are regulated in part by events that are connected to the emergence and extension of the primitive streak (Forlani et al., 2003; Iimura and Pourquie, 2006). A contribution of RA signaling to the initial activation of *Hox* expression has been suggested, since at early developmental stages, embryos with impaired RA synthesis (*Raldh2*$^{-/-}$ mutants) exhibit abnormal initial 3′ *Hox* gene expression domains (Niederreither et al.,

1999). Moreover, RA was shown to regulate embryonic AP patterning, in particular by controlling the expression of specific *Hox* genes (Niederreither and Dolle, 2008; Alexander et al., 2009).

In this study, we show that the anterior *Hox* genes, *Hoxb1*, *Hoxa1* and *Hoxa3*, are expressed in the SHF as early as embryonic day (E) 7.5 and define distinct sub-domains in the splanchnic mesoderm. Genetic (cre-mediated) lineage tracing reveals that *Hoxb1*, *Hoxa1* and *Hoxa3*-expressing cardiac progenitor cells give rise to the atria and the inferior wall of the OFT, which subsequently yields the myocardium at the base of the pulmonary trunk. Furthermore, $Hoxb1^{IRES\text{-}Cre}$, *Hoxa1-enhIII-Cre* and $Hoxa3^{IRES\text{-}Cre}$ marked cells shows differential contributions to the proximal and distal regions of the OFT. Manipulation of the RA signaling pathway using $Raldh2^{-/-}$ embryos or injection of all-*trans*-RA demonstrates that expression of these *Hox* genes in the SHF and their cardiac contribution to the heart are sensitive to RA dosage. Comparison of transgenes expression in *Raldh2* mutant embryos reveals that RA signaling is required for these *Hox*-expressing cardiac progenitor cell populations to contribute to the heart.

MATERIALS AND METHODS

Mouse lines and breeding

All mouse lines used in this study have been previously described: *Raldh2*-null (Niederreither et al., 1999), $Hoxa3^{IRES\text{-}Cre}$ (Macatee et al., 2003), $Hoxb1^{IRES\text{-}Cre}$ (Arenkiel et al., 2003), alleles and $Mlc1v\text{-}nlacZ\text{-}24/Fgf10^{lacZ}$ (Kelly et al., 2001), *RARE-hsp68-lacZ* (Rossant et al., 1991), *y96-Myf5-nlacZ-16* (*96-16*), *A17-Myf5-nlacZ-T55* (*T55*) (Bajolle et al., 2008) and *R26R-lacZ* (Soriano, 1999) transgenes. Mice were genotyped by PCR as described in the original reports. Embryos were staged taking embryonic day (E) 0.5 as the morning of the vaginal plug. Cre-induced recombination was analyzed by breeding Cre mice with *R26R-lacZ* reporter mice and analyzing embryos with the genotype *Cre; R26R-lacZ* by X-gal staining. Animal care was in accordance with national and institutional guidelines.

Generation of novel transgenic line

The *Hoxa1* enhancer III-Cre (*Hoxa1-enhIII-Cre*) construct DNA was previously described by Li and Lufkin (2000) (Li and Lufkin, 2000). Transgenic mice were generated by microinjection of purified plasmid DNA into fertilized (C57BL/6XDBA/2) F_2 eggs at a concentration of approx. 1ng/ul using standard techniques. Injected eggs were re-implanted the day after the injection into pseudo-pregnant (C57BL/6), foster mothers.

X-gal staining, histology and RNA in situ hybridizations

To visualize β-galactosidase activity, embryos or hearts were isolated, fixed in 4% paraformaldehyde for 20min and moved into X-gal solution, according to standard procedures. Embryos or hearts were photographed (Zeiss Lumar V12 stereomicroscope) as whole-mount specimens and then embedded in O.C.T. and cut into 12μM histological section before being counterstained with eosin.

Whole-mount *in situ* hybridization (ISH) was performed as previously described (Ryckebusch et al., 2008). Double whole-mount ISH with digoxigenin (DIG)- and FITC-labeled riboprobes were performed according to the Stern laboratory protocol (http://www.ucl.ac.uk/cdb/research/stern/stern_lab/insitu, Protocols section).

The following riboprobes used in this study were *Bmp4*, *Hoxa1*, *Hoxb1*, *Hoxa2*, *Hoxa3*, *islet1*, *Tbx5*, *Raldh2*, and *Wnt11*. For single ISH, hybridization signals were then detected by alkalin phosphatase (AP)-conjugated anti-DIG antibodies (1/2000; Roche), which were

followed by color development with NBT/BCIP (magenta) substrate (Promega). For double ISH hybridization signals we used an anti-FITC antibody coupled to AP (1/2000; Roche), and the NBT-BCIP (magenta) (promega) for the first detection, and an anti-DIG antibody coupled to AP (1/2000; Roche) and the INT-BCIP (brick red) (Roche) for the second detection. After staining, the samples were washed in PBS and post-fixed. Embryos were photographed using a Zeiss Lumar stereomicroscope coupled to an Axiocam digital camera (AxioVision 4.4, Zeiss). The number of embryos examined was at least 3 for each stage.

Immunostaining

Embryos were fixed at 4°C for 20min in 4% paraformaldehyde, rinsed in PBS, equilibrated to 15% sucrose and embedded in O.C.T. Cryosections were cut at 12μm, washed in PBS and pre-incubated in blocking solution (1%BSA, 1% Serum, 0.2% Tween20 in PBS). Primary antibodies were applied overnight at 4°C, followed by secondary detection using Alexa Fluor conjugated (Molecular Probes) secondary antibodies. Sections were photographed using Leica DM 5000B microscope.

The following primary antibodies were used in this study: rabbit anti-Hoxb1 (Covance; 1/200), rabbit anti-GFP (Invitrogen; 1/500), rabbit anti-βGal (sigma; 1/500) and mouse anti-Islet1 (DSHB: 1/100).

Retinoic acid treatment of embryos

All-*trans*-RA (Sigma) was dissolved in DMSO and diluted at 20mg/ml. At E7.75, the mice were given a single intra-peritoneal injection of RA (70mg/kg or 85mg/kg) or control DMSO. Embryos were later dissected at E8.5 or E9.5.

RESULTS

Anterior-posterior patterning of the second heart field

We previously reported that RA signaling is required to establish the posterior limit of the second heart field (SHF) in splanchnic mesoderm of mouse embryos (Ryckebusch et al., 2008). However, this study did not identify the molecules downstream of RA signaling that are responsible for the restriction of cardiac progenitors. *Hox* genes have been suggested to be among the key downstream effectors of RA signaling during cardiac patterning (Searcy and Yutzey, 1998; Waxman et al., 2008). Therefore, we examined the expression pattern of several *Hox* genes within the lateral mesoderm and compared their expression to cardiac markers. We selected *Hoxb1, Hoxa1* and *Hoxa3* because they are among the first *Hox* genes to be activated at the primitive streak and consequently display anterior limits of expression close to the cardiac field. At E7.25, the expression domains of *Hoxb1, Hoxa1* and *Hoxa3* overlapped with those of the RA-synthesizing enzyme *Raldh2*, and the *RARE-lacZ* transgene, a reporter for RA activity (Supplemental Fig. S1). During extension of the primitive streak, transcription of *Hoxb1* initiates earlier than *Hoxa1* and *Hoxa3* (Supplemental Fig. S1), suggesting that sequential temporal activation of these *Hox* genes is important to establish anterior-posterior (AP) patterning of the lateral mesoderm. At E7.75, the anterior border of *Hoxb1* expression is more rostral than those of *Hoxa1* and *Hoxa3* (Fig. 1A,D,G).

Despite reported expression in early mesodermal cells (Frohman et al., 1990; Murphy and Hill, 1991), *Hox* gene expression relative to the heart field has never been explored in the mouse. To assess the expression of *Hox* genes in the heart field, we performed double *in situ* hybridization with *Tbx5* and *Islet1* (*Isl1*), which label the cardiac crescent and the SHF respectively (Fig. 1H,I) (Buckingham et al., 2005). At the early cardiac crescent stage, *Hoxb1* (orange) and *Isl1* (purple) exhibit an overlap of their expression domains (compare

Fig. 1A,C and I; arrowheads), suggesting that *Hoxb1* is expressed in cardiac progenitor cells. Embryos double-stained for *Hoxb1* and *Tbx5* (purple) display no overlap, indicating that *Hoxb1* is not expressed in *Tbx5*-positive cells (compare Fig. 1A,B and H). Consistent with our previous observations (Ryckebusch et al., 2008), double labeling confirms that the *Hoxa1* expression domain is adjacent to the cardiogenic region marked by *Tbx5* at E7.75 (Fig. 1E). However, we detected a small overlap between *Hoxa1* and *Isl1* in the splanchnic mesoderm (compare Fig. 1D,F and I, arrowheads). As the heart tube forms, *Hoxb1* and *Hoxa1* are expressed in both the splanchnic mesoderm and the ventral and lateral foregut endoderm, but not in the heart tube (Fig. 2A,C), as confirmed by double *in situ* hybridization with *Isl1* (Supplemental Fig. S2). Double immunohistochemistry for Hoxb1 and Isl1 revealed that Hoxb1 and Isl1-positive nuclei co-localize in the caudal region of the SHF (Supplemental Fig. S3), suggesting that Hoxb1 expression characterizes a sub-domain of the $Isl1^{+}$ splanchnic mesodermal population.

In order to examine the anterior boundaries of the expression of these *Hox* genes within the splanchnic mesoderm, we used *Mlc1v-nlacZ-24 (Mlc1v-24*) transgenic mice, in which a transgene integration at the *Fgf10* locus leads to β-galactosidase expression in the anterior domain of the SHF, referred to as the anterior heart field (AHF) (Kelly et al., 2001). We thus found that *Hoxb1* transcripts and β-galactosidase activity co-localize in the posterior half region of the AHF (Fig. 2A,B). Co-localization of *Hoxa1* expression and *Mlc1-nlacZ-v24* staining is more limited, since it is observed only in the most caudal margin of the AHF (Fig. 2C,D), suggesting that the anterior limit of the expression domain of *Hoxa1* is within the posterior region of the AHF. In contrast, *Hoxa3* expression is not detected in the AHF but in splanchnic mesoderm located posteriorly to the heart tube region (Fig. 2E,F). Taken together, these results show that *Hoxb1* and *Hoxa1* are expressed in the SHF with different anterior limits of expression within the caudal AHF, while *Hoxa3* is essentially expressed in the most caudal region of the posterior SHF. Importantly, *Hoxb1*, *Hoxa1* and *Hoxa3* transcripts were not detected in differentiated cardiomyocytes.

Hoxb1-expressing cardiac progenitor cells contribute to the inferior wall of the outflow tract

Recent evidence suggests that posterior SHF contributes to the atria in mice (Cai et al., 2003; Galli et al., 2008), whereas the AHF gives rise to the OFT and the right ventricle (Kelly et al., 2001; Zaffran et al., 2004). Our *in situ* hybridization analysis suggests that $Hoxb1^{+}$ cardiac progenitor cells might thereby contribute to both the arterial and venous poles of the heart. To investigate this question, we performed genetic lineage tracing analysis of *Hoxb1*-expressing cells by crossing a $Hoxb1^{IRES\text{-}Cre}$ allele (Arenkiel et al., 2003) with the *R26R-lacZ* reporter line (Soriano, 1999), which expresses β-galactosidase upon Cre recombination. Until E7.75, the recombination pattern in lateral mesoderm of $Hoxb1^{IRES\text{-}Cre}$; *R26R-lacZ* embryos was highly similar to the expression pattern of *Hoxb1*, including their anterior boundary (Supplemental Fig. S4). At E8.5, however, the pattern of recombination in $Hoxb1^{IRES\text{-}Cre}$; *R26R-lacZ* embryos was discordant with that of *Hoxb1* expression. *Hoxb1*, or *Cre*, transcripts were confined to the SHF, whereas β-galactosidase activity was found in the venous pole of the heart (Supplemental Fig. S4). Between E9 and E16.5, *Hoxb1* expression was not detected in differentiated cardiomyocytes (data not shown), whereas β-galactosidase activity was found in the majority of the atrial cells and the atrioventricular canal (AVC) myocardium and its derivatives, including the atrioventricular valves (Fig. 3A,C,G). X-gal stained cells were found in the working myocardium of the left ventricular free wall contiguous with AVC derivatives (Fig. 3G), confirming that the AVC lineage provides a contribution to this region of the left ventricle (Aanhaanen et al., 2009). However, this contribution is less important than the one observed for $Tbx2^{+}$ progeny by Aanhaanen et al. β-galactosidase activity was also detected in the epicardium (Fig. 3E–H)

and subsequently in the walls of the main coronary vessels (Fig. 3H; arrowhead). Because *Raldh2* is strongly expressed in the proepicardium (Moss et al., 1998; Xavier-Neto et al., 1999) and RA signaling has an established function in the fetal epicardium (Merki et al., 2005; Lin et al., 2010), we cannot exclude later activation of *Hoxb1* in this tissue. This contribution is also observed in postnatal heart (data not shown).

At E9 and E10.5, descendants of cells expressing *Hoxb1* are also observed in the arterial pole (Fig. 3B) and in the OFT of *Hoxb1*$^{IRES\text{-}Cre}$; *R26R-lacZ* embryos (Fig. 3D). X-gal labeled cells are detected exclusively in the inferior wall of the OFT (Fig. 3D). Between E11.5 and E16.5, β-galactosidase activity is found in the left side of the OFT wall and then in the myocardium at the base of the pulmonary trunk (Fig. 3E,F,H), but not at the base of the aorta (Fig. 3I). This confirms that the myocardial wall of the OFT rotates as previously suggested (Bajolle et al., 2006). Together, these findings indicate that precursors of the inferior wall of the OFT, which contribute to the base of the pulmonary trunk, segregate early in the SHF as proposed from a previous study of regionalized transgene expression and retrospective clonal analysis (Bajolle et al., 2008).

Our *in situ* hybridization analysis revealed a spatial difference between *Hoxb1*, *Hoxa1* and *Hoxa3* transcripts in the SHF (Fig. 2). To compare the contribution of *Hoxa1*- and *Hoxa3*-expressing cells with the *Hoxb1*-lineage, we performed genetic lineage tracing using a *Hoxa1-enhIII-Cre* transgene (Li and Lufkin, 2000) and a *Hoxa3*$^{IRES\text{-}Cre}$ allele (Macatee et al., 2003). We used the 0.5kb *Hoxa1* enhancer III because it was reported to recapitulate a significant portion of the *Hoxa1* expression domain and to contain a functional RA regulatory element (RARE) (Frasch et al., 1995). Until E8 to E9.5, the pattern of recombination in *Hoxa1-enhIII-Cre; R26R-lacZ* embryos was highly similar to the expression pattern of *Hoxa1* (Supplemental Fig. S5). At E9.5, X-gal staining revealed minimal difference to that seen with *Hoxa1*$^{IRES\text{-}Cre}$; *R26R-lacZ* embryos at the same stage (Supplemental Fig. S5), as recently described (Makki and Capecchi, 2010). This supports the use of the *Hoxa1-enhIII-Cre* transgene for our lineage analyses. Between E10.5 and E16.5, descendants of cells expressing *Hoxa1* were observed in a small number of atrial cells in *Hoxa1-enhIII-Cre; R26R-lacZ* embryos (Fig. 4A–D). Of note, X-gal-labeled cells were never found in the AVC in these embryos (data not shown), suggesting that AVC myocytes are derived from the *Hoxb1*-lineage but not the *Hoxa1*-lineage. As in *Hoxb1*$^{IRES\text{-}Cre}$; *R26R-lacZ* hearts, X-gal-labeled cells in the *Hoxa1-enhIII*-lineage were located in the inferior wall of the OFT (Fig. 4A,B). In contrast, β-galactosidase activity was only detected in the distal OFT of *Hoxa1-enhIII-Cre; R26R-lacZ* embryos (Fig. 4A,B), consistent with the small number of X-gal-labeled cells found later in the myocardium at the base of the pulmonary trunk (Fig. 4C,D). At E12.5, the *Hoxa1-enhIII* labeled cells were seen in the cushions of the OFT (Fig. 4C), which probably corresponds to recombination in neural crest cells.

Our *Hoxa3*$^{+}$ lineage analysis confirms that *Hoxa3*$^{IRES\text{-}Cre}$ recombination in the pharyngeal region begins at E8 in surface ectoderm (Supplemental Fig. S5), and then extends into pharyngeal endoderm and mesoderm (Macatee et al., 2003; Zhang et al., 2005). The recombination pattern in *Hoxa3*$^{IRES\text{-}Cre}$; *R26R-lacZ* embryos recapitulated the caudal to rostral progression of *Hoxa3* expression (Supplemental Fig. S1 and Fig. S5). Consistent with the other *Hox* lineages, β-galactosidase activity was detected in the inferior myocardial wall of the distal OFT of *Hoxa3*$^{IRES\text{-}Cre}$; *R26R-lacZ* embryos (Fig. 4E,F). Subsequently, X-gal staining was observed in myocardium at the base of the pulmonary trunk (Fig. 4H). We also found X-gal labeled cells in the OFT cushions (Fig. 4G). Together our findings suggest that spatial differences between *Hoxb1*, Hoxa1 and *Hoxa3* observed in the splanchnic mesoderm at E8.5 (Fig. 2) identify overlapping populations of cardiac progenitor cells that contribute differentially to the proximal and distal regions of the OFT (Fig. 3 and 4).

Reduction or excess of RA signaling alter the Hoxa1- and Hoxb1-lineages

The homeobox genes *Hoxa1* and *Hoxb1* are known to be RA-regulated both *in vitro* and *in vivo* via RA-response elements (RAREs) present in their regulatory regions (Marshall et al., 1996; Langston et al., 1997; Studer et al., 1998; Niederreither et al., 1999; Huang et al., 2002; Sirbu et al., 2005). Our *Hoxa1* and *Hoxb1* genetic lineage analysis also shows similarities with the RA-activated cell lineages recently described by Dollé et al. (Dolle et al., 2010) and Li et al. (Li et al., 2010). This raises the possibility that a deficiency in RA biosynthesis might affect the *Hox* lineages. To address this question, we examined *Hoxa1* and *Hoxb1* expression patterns in embryos deficient in RA synthesis. We found that expression of *Hoxa1* and *Hoxb1*, as well as *Hoxa3*, are downregulated in the splanchnic mesoderm at E8.5 in *Raldh2*$^{-/-}$ embryos (Supplemental Fig. S6). We next examined *Hoxb1*$^{IRES\text{-}Cre}$ and *Hoxa1-enhIII-Cre* lineages in *Raldh2*$^{-/-}$ embryos. At E8.5 and E9.5, there is no X-gal staining in *Hoxa1-enhIII-Cre; R26R-lacZ; Raldh2*$^{-/-}$ embryos (Fig. 5A-C). This observation supports the importance of signaling through the RA regulatory element (RARE) present in *Hoxa1* enhancer III (Frasch et al., 1995; Li and Lufkin, 2000). In contrast to the *Hoxa1-enhIII-Cre* lineage, β-galactosidase positive cells were still detected in *Hoxb1*$^{IRES\text{-}Cre}$; *R26R-lacZ; Raldh2*$^{-/-}$ embryos (Fig. 5D–F), suggesting that early expression of *Hoxb1* in cardiac progenitor cells may not be activated by RA signaling. However, sections show that β-galactosidase activity was also not visible in the ectoderm of *Raldh2*$^{-/-}$ embryos (Fig. 5E,F), revealing tissue-specific sensitivity to RA signaling. Although the *Hoxb1*$^{IRES\text{-}Cre}$ lineage was detectable in *Raldh2*$^{-/-}$ mutant hearts, we believe that incorporation of X-gal labeled cells into the heart tube may be a consequence of the lack of the dorsal closure of the heart tube rather than a normal addition process at both the arterial and venous poles (Fig. 5F).

To determine whether *Hox*-lineages are sensitive to increased RA signaling, we treated the mothers of *Hoxa1-enhIII-Cre; R26R-lacZ* and *Hoxb1*$^{IRES\text{-}Cre}$; *R26R-lacZ* embryos with a teratogenic dose of RA to disrupt the normal boundary of RA activity (Niederreither et al., 1999; Sirbu et al., 2005). When we administrated a 70mg/kg dose of RA at E7.75, we confirmed the anterior shift of the rostral border of *Hoxa1*, *Hoxb1* and *Hoxa3* expression domains, including in the pharyngeal mesoderm (Supplemental Fig. S6). Consistently, comparison of control and RA-treated *Hoxb1*$^{IRES\text{-}Cre}$; *R26R-lacZ* embryos demonstrated that the *Hoxb1*$^{IRES\text{-}Cre}$ lineage is responsive to RA (Fig. 5I,J). Importantly, X-gal labeled cells were found in the forming heart tube (Fig. 5J,J′), suggesting that the anterior boundary of RA activity defines the location of the *Hoxb1*$^{IRES\text{-}Cre}$ lineage boundary. Effect of RA-treatment on *Hoxa1-enhIII-Cre; R26R-lacZ* embryos was weaker (Fig. 5G,H), suggesting that the RARE within enhancer III-Cre transgene is less sensitive than in the context of the endogenous *Hoxa1* promoter. When a 85mg/kg dose of RA was injected at E8.5 in *Hoxa3*$^{IRES\text{-}Cre}$; *R26R-lacZ* embryos, only few X-gal labeled cells were found anterior to the otic vesicle and in the first branchial arch (Supplemental Fig. S7), suggesting that RA has a restricted effect on the activation of the *Hoxa3*-lineage after E8.

Our previous and present results showed that RA is required for correct deployment of the SHF (Ryckebusch et al., 2008). In addition, a recent study suggested that formation of the OFT is disrupted in RA receptor mutant embryos, resulting in a short, misaligned OFT (Li et al., 2010). To further explore the role of RA signaling on OFT formation, we compared the expression of *y96-Myf5-nlacZ-16* (*96-16*) and *A17-Myf5-nlacZ-T55* (*T55*) transgenes (Bajolle et al., 2006; Bajolle et al., 2008), which have complementary patterns in the OFT, in *Raldh2*$^{-/-}$ mutant embryos. Interestingly, the domain of expression of the *96-16* transgene corresponded to the β-galactosidase activity observed in the OFT in *Hoxb1*$^{IRES\text{-}Cre}$; *R26R-lacZ* embryos (Fig. 6A and Fig. 3D). Thus, we found that the sub-domain of *96-16* transgene expressing cells is missing in the RA deficient embryos (Fig. 6A,B), whereas cells expressing the *T55* transgene were still present in the OFT of

Raldh2$^{-/-}$ mutant hearts (Fig. 6C,D). These results suggest that only a sub-domain of the OFT is affected in *Raldh2*$^{-/-}$ mutant embryos. We presume that perturbation of RA signaling causes a failure in the deployment of the *Hoxb1*-expressing cardiac progenitor cell subpopulation during the formation of the OFT.

DISCUSSION

Anterior-posterior patterning of the SHF in the mouse

Previous expression and genetic lineage studies indicated that the majority of cardiac components (outflow tract [OFT], right ventricular and atrial myocardium) are derived from an *Isl1*$^{+}$ splanchnic mesodermal cell population, called the second heart field (SHF) (Cai et al., 2003; Ma et al., 2008). The question of the early spatial segregation of cardiac progenitor cells is crucial to understand their specification in precardiac mesoderm and subsequent fate in the heart. There is increasing evidence for the existence of cardiac progenitor sub-populations in the SHF, such as the anterior region of the SHF (also called AHF and marked by expression of *Fgf10*) (Kelly et al., 2001), which contributes to right ventricular and OFT myocardium (Zaffran et al., 2004), whereas the posterior SHF, which expresses *Isl1* but not *Fgf10*, contributes to atrial myocardium (Cai et al., 2003; Galli et al., 2008). These observations indicate that at least two sub-compartments are positioned along the AP axis within the SHF. Our data reveal that expression of *Hox* genes characterizes distinct progenitor cell sub-domains within the SHF. These results suggest that regionalized expression of *Hoxb1* and *Hoxa1* in splanchnic mesoderm may be required to establish AP patterning of the SHF. Furthermore, our genetic lineage tracing analysis shows that *Hoxb1, Hoxa1 and Hoxa3* lineages contribute to both the arterial and venous poles of the heart (Fig. 7). Contribution of *Hoxa1* and *Hoxa3* lineages to the OFT supports the idea that posterior SHF cells might contribute the arterial pole of the forming heart tube. Interestingly, we observed a difference in the contribution of *Hox* lineages to the proximo-distal region of the OFT and atria; descendants of cells expressing *Hoxb1* are found in the proximal OFT and atria, while descendants of cells expressing *Hoxa1* and *Hoxa3* are observed only in the distal OFT and in discrete regions of the atria. These results indicate that segregation among cardiac progenitor cells occurs before their incorporation to the arterial and venous poles of the heart. Interestingly, retrospective clonal analysis in the heart at E8.5 has identified clones that can contribute to regions of both the future atria and OFT (Meilhac et al., 2004). Thus, we believe that these clones are born from *Hoxb1*$^{+}$ progenitor cells.

Hox genes have been proposed to be the key downstream effectors of RA signaling during cardiac development (reviewed in (Rosenthal and Xavier-Neto, 2000)). This is supported by recent studies in zebrafish, which identified *Hoxb5b* as a downstream target of RA signaling that restricts the numbers of both atrial and ventricular cells that emerge from the heart field (Waxman et al., 2008), and showed that injection of *Hoxb5b* mRNA phenocopies RA treatment, which consists in the loss of both atrial and ventricular cardiomyocytes (Waxman and Yelon, 2009). Waxman et al. have shown that reduction of RA signaling does not lead to an increase in ventricular cells at the expense of the atrial lineage (Waxman et al., 2008). These observations are not consistent with a role for RA signaling in partitioning the heart tube, as suggested by previous studies in amniotes (Yutzey et al., 1994; Hochgreb et al., 2003; Ryckebusch et al., 2008; Sirbu et al., 2008). Indeed, treatment of chick embryos with a RA pan-antagonist produces a heart with reduction of the atrial compartment and an oversized ventricle (Hochgreb et al., 2003), while RA deficiency mouse embryos have impaired atrial and sinus venosus development (Niederreither et al., 2001), as well as loss of the inferior wall of the OFT (this study). We have shown that manipulation of RA signaling affects the rostral boundaries of *Hoxa1, Hoxb1* and *Hoxa3* expression in the SHF. Therefore, RA may control AP patterning of the SHF through the tight regulation of the expression of these *Hox* genes in splanchnic mesoderm. The question of the role of anterior *Hox* genes in

the SHF can only be determined by inactivating and overexpressing these genes in their respective precursor populations. Of note, no abnormality in the heart of *Hoxa1 and Hoxb1* mutant mice have been reported (Lufkin et al., 1991; Carpenter et al., 1993; Goddard et al., 1996; Studer et al., 1996), but non-lethal cardiovascular morphological defects may not have been examined in detail. Moreover, *Hoxa1* and *Hoxb1* have been shown to function together in several structures including the hindbrain, cranial nerves and second pharyngeal arch (Gavalas et al., 1998; Studer et al., 1998; Rossel and Capecchi, 1999). Hence, characterization of cardiac defects in double *Hoxa1;Hoxb1* homozygous mutant embryos will be essential.

Contribution of Hox lineages to the outflow tract of the heart

Diverse subpopulations of the SHF have been defined in the mouse and chick. These include the anterior heart field (AHF), giving rise to all OFT myocardium, and the “secondary” heart field, situated in the dorsal pericardial wall giving rise to myocardium of the distal OFT (Kelly et al., 2001; Mjaatvedt et al., 2001; Waldo et al., 2001). Our results indicate that the splanchnic mesodermal cells expressing *Hoxa1* are part of the murine “secondary” heart field. Surprisingly, our findings show that cardiac progenitor cells expressing *Hoxb1*, *Hoxa1* and *Hoxa3* contribute to sub-pulmonary myocardium but not myocardial cells at the base of the aorta. This is consistent with observations on the clustering of clonally related cells in the OFT (Bajolle et al., 2008), which had suggested that future sub-pulmonary myocardium is pre-patterned in distinct sub-domains of progenitor cells. Future sub-aortic myocardial progenitor cells are positioned anterior to future sub-pulmonary progenitor cells in the SHF. Interestingly, the contribution of *Hoxb1*-expressing cardiac progenitor cells to the OFT is very similar to that of $Tbx1^{Cre}$ at E10.5 (Huynh et al., 2007). Deletion of *Tbx1*, the major candidate gene for DiGeorge syndrome, results in a persistent truncus arteriosus (PTA) (Baldini, 2005), and sub-pulmonary myocardium is specifically affected in *Tbx1* mutant hearts (Theveniau-Ruissy et al., 2008). Thus, it will be of interest to explore the contribution of the *Hoxb1*-lineage in the absence of *Tbx1*.

Studies on RA receptors (*RARα1/RARβ/RXRα*) and *Raldh2* mutant embryos have demonstrated the importance of RA signaling during OFT development (Lee et al., 1997; Niederreither et al., 2001; Jiang et al., 2002; Li et al., 2010). Interestingly, results from RAR mutants imply that proximal and distal domains of the OFT are pre-patterned in the splanchnic mesoderm (Li et al., 2010), consistent with the differential AP expression of *Hoxb1*, *Hoxa1* and *Hoxa3* in the SHF, and their different contributions to the OFT. Thus, we hypothesize that the SHF is patterned from anterior to posterior, as follows: cells giving rise to the right ventricle and superior wall of the OFT (*Hox*-negative cells), to the inferior wall of the proximal OFT (*Hoxb1*-positive cells), to the inferior wall of the distal OFT (*Hoxb1* and *Hoxa1*-positive cells), and, most posteriorly, to atrial myocardium. Analysis of RA synthesis and RA response suggest that RA signaling acts predominantly in SHF cells characterized by *Hoxb1* expression (Moss et al., 1998; Hochgreb et al., 2003; Ryckebusch et al., 2008; Sirbu et al., 2008; Dolle et al., 2010). This is supported by analysis of *Raldh2* and RA receptor mutants in which derivatives of $Hoxb1^{+}$ sub-domains as described above are lacking (Ryckebusch et al., 2008; Li et al., 2010 and this study). OFT defects observed in RA receptor mutants as well as in RA-rescued *Raldh2* mutants, suggest that RA signaling acts from E7.5 to E10.5 to allow correct deployment of $Hoxb1^{+}$ progenitor cells (Niederreither et al., 2001; Li et al., 2010). Works performed on $Raldh2^{-/-}$ mutants have shown that RA signaling is required first to determine the posterior limit of the SHF as posterior expansion of SHF markers is observed as soon as E7.5 (Ryckebusch et al., 2008; Sirbu et al., 2008). Maternal RA supplementation experiments reveal a further requirement of RA until E10.5 that we believe is associated with contribution of $Hoxb1^{+}$ progenitor cells to the heart tube (Niederreither et al., 2001). RA could allow this contribution through

controlling specification, differentiation and/or migration of those SHF cells. With respect to absent septation and misalignments of the OFT including PTA, double outlet right ventricle (DORV) and overriding aorta observed in RA receptor and RA-rescued *Raldh2* mutant embryos (Niederreither et al., 2001; Li et al., 2010), we speculate that lack of the inferior wall of the OFT, a derivative of particular *Hoxb1*$^{+}$ progenitor cells, may be sufficient to lead to these defects. Of course, the latter speculation does not exclude a potential role of RA signaling on cardiac NCC (Niederreither et al., 2001; Jiang et al., 2002).

In human congenital heart disease, OFT alignment defects, such as tetralogy of Fallot, are frequent and may result from a deficit in sub-pulmonary myocardium (Van Praagh, 2009). It is interesting to note that recent studies in humans have identified homozygous *HOXA1* coding mutations in patients with OFT defects, including tetralogy of Fallot (Tischfield et al., 2005; Bosley et al., 2008). Together with our present results, these observations should lead to further investigations into the causative role of *HOX* mutations in the pathogenesis of heart and great vessels malformations in humans.

Supplementary Material

Refer to Web version on PubMed Central for supplementary material.

Acknowledgments

We thank T. Lufkin for the *Hoxa1* Enhancer III-Cre vector and members of the SEAT CNRS UPS44 mouse facility for microinjection. This manuscript was improved by helpful comments from M. Buckingham, H. Etchevers and R.G. Kelly. This work is supported by the “Agence Nationale de la Recherche” (ANR-07-MRAR-003), (to S.Z), the “Association Française contre les Myopathies” (AFM 13517 and 14134) (to S.Z.), and the National Institutes of Health (R01 HL070733) (to K.N.). L.R. and M.R. received fellowships from the “Ministère de l’Enseignement Supérieur et de la Recherche” and the “Université de la Méditerranée” (Monitorat).

References

Aanhaanen WT, Brons JF, Dominguez JN, Rana MS, Norden J, Airik R, Wakker V, de Gier-de Vries C, Brown NA, Kispert A, Moorman AF, Christoffels VM. The Tbx2+ primary myocardium of the atrioventricular canal forms the atrioventricular node and the base of the left ventricle. Circ Res. 2009; 104:1267–1274. [PubMed: 19423846]

Alexander T, Nolte C, Krumlauf R. Hox genes and segmentation of the hindbrain and axial skeleton. Annu Rev Cell Dev Biol. 2009; 25:431–456. [PubMed: 19575673]

Arenkiel BR, Gaufo GO, Capecchi MR. Hoxb1 neural crest preferentially form glia of the PNS. Dev Dyn. 2003; 227:379–386. [PubMed: 12815623]

Bajolle F, Zaffran S, Kelly RG, Hadchouel J, Bonnet D, Brown NA, Buckingham ME. Rotation of the myocardial wall of the outflow tract is implicated in the normal positioning of the great arteries. Circ Res. 2006; 98:421–428. [PubMed: 16397144]

Bajolle F, Zaffran S, Meilhac SM, Dandonneau M, Chang T, Kelly RG, Buckingham ME. Myocardium at the base of the aorta and pulmonary trunk is prefigured in the outflow tract of the heart and in subdomains of the second heart field. Dev Biol. 2008; 313:25–34. [PubMed: 18005956]

Baldini A. Dissecting contiguous gene defects: TBX1. Curr Opin Genet Dev. 2005; 15:279–284. [PubMed: 15917203]

Bosley TM, Alorainy IA, Salih MA, Aldhalaan HM, Abu-Amero KK, Oystreck DT, Tischfield MA, Engle EC, Erickson RP. The clinical spectrum of homozygous HOXA1 mutations. Am J Med Genet A. 2008; 146A:1235–1240. [PubMed: 18412118]

Buckingham M, Meilhac S, Zaffran S. Building the mammalian heart from two sources of myocardial cells. Nat Rev Genet. 2005; 6:826–835. [PubMed: 16304598]

Cai CL, Liang X, Shi Y, Chu PH, Pfaff SL, Chen J, Evans S. Isl1 identifies a cardiac progenitor population that proliferates prior to differentiation and contributes a majority of cells to the heart. Dev Cell. 2003; 5:877–889. [PubMed: 14667410]

Carpenter EM, Goddard JM, Chisaka O, Manley NR, Capecchi MR. Loss of Hox-A1 (Hox-1.6) function results in the reorganization of the murine hindbrain. Development. 1993; 118:1063–1075. [PubMed: 7903632]

Dolle P, Fraulob V, Gallego-Llamas J, Vermot J, Niederreither K. Fate of retinoic acid-activated embryonic cell lineages. Dev Dyn. 2010; 239:3260–3274. [PubMed: 21046629]

Duboule D, Dolle P. The structural and functional organization of the murine HOX gene family resembles that of Drosophila homeotic genes. Embo J. 1989; 8:1497–1505. [PubMed: 2569969]

Forlani S, Lawson KA, Deschamps J. Acquisition of Hox codes during gastrulation and axial elongation in the mouse embryo. Development. 2003; 130:3807–3819. [PubMed: 12835396]

Frasch M, Chen X, Lufkin T. Evolutionary-conserved enhancers direct region-specific expression of the murine Hoxa-1 and Hoxa-2 loci in both mice and Drosophila. Development. 1995; 121:957–974. [PubMed: 7743939]

Frohman MA, Boyle M, Martin GR. Isolation of the mouse Hox-2.9 gene; analysis of embryonic expression suggests that positional information along the anterior-posterior axis is specified by mesoderm. Development. 1990; 110:589–607. [PubMed: 1983472]

Galli D, Dominguez JN, Zaffran S, Munk A, Brown NA, Buckingham ME. Atrial myocardium derives from the posterior region of the second heart field, which acquires left-right identity as Pitx2c is expressed. Development. 2008; 135:1157–1167. [PubMed: 18272591]

Gaufo GO, Flodby P, Capecchi MR. Hoxb1 controls effectors of sonic hedgehog and Mash1 signaling pathways. Development. 2000; 127:5343–5354. [PubMed: 11076756]

Gavalas A, Studer M, Lumsden A, Rijli FM, Krumlauf R, Chambon P. Hoxa1 and Hoxb1 synergize in patterning the hindbrain, cranial nerves and second pharyngeal arch. Development. 1998; 125:1123–1136. [PubMed: 9463359]

Goddard JM, Rossel M, Manley NR, Capecchi MR. Mice with targeted disruption of Hoxb-1 fail to form the motor nucleus of the VIIth nerve. Development. 1996; 122:3217–3228. [PubMed: 8898234]

Graham A, Papalopulu N, Krumlauf R. The murine and Drosophila homeobox gene complexes have common features of organization and expression. Cell. 1989; 57:367–378. [PubMed: 2566383]

Hochgreb T, Linhares VL, Menezes DC, Sampaio AC, Yan CY, Cardoso WV, Rosenthal N, Xavier-Neto J. A caudorostral wave of RALDH2 conveys anteroposterior information to the cardiac field. Development. 2003; 130:5363–5374. [PubMed: 13129847]

Huang D, Chen SW, Gudas LJ. Analysis of two distinct retinoic acid response elements in the homeobox gene Hoxb1 in transgenic mice. Dev Dyn. 2002; 223:353–370. [PubMed: 11891985]

Huynh T, Chen L, Terrell P, Baldini A. A fate map of Tbx1 expressing cells reveals heterogeneity in the second cardiac field. Genesis. 2007; 45:470–475. [PubMed: 17610275]

Iimura T, Pourquie O. Collinear activation of Hoxb genes during gastrulation is linked to mesoderm cell ingression. Nature. 2006; 442:568–571. [PubMed: 16760928]

Izpisua-Belmonte JC, Dolle P, Renucci A, Zappavigna V, Falkenstein H, Duboule D. Primary structure and embryonic expression pattern of the mouse Hox-4.3 homeobox gene. Development. 1990; 110:733–745. [PubMed: 1982431]

Jiang X, Choudhary B, Merki E, Chien KR, Maxson RE, Sucov HM. Normal fate and altered function of the cardiac neural crest cell lineage in retinoic acid receptor mutant embryos. Mech Dev. 2002; 117:115–122. [PubMed: 12204252]

Keegan BR, Feldman JL, Begemann G, Ingham PW, Yelon D. Retinoic acid signaling restricts the cardiac progenitor pool. Science. 2005; 307:247–249. [PubMed: 15653502]

Kelly RG, Brown NA, Buckingham ME. The arterial pole of the mouse heart forms from Fgf10-expressing cells in pharyngeal mesoderm. Dev Cell. 2001; 1:435–440. [PubMed: 11702954]

Langston AW, Thompson JR, Gudas LJ. Retinoic acid-responsive enhancers located 3′ of the Hox A and Hox B homeobox gene clusters. Functional analysis. J Biol Chem. 1997; 272:2167–2175. [PubMed: 8999919]

Lee RY, Luo J, Evans RM, Giguere V, Sucov HM. Compartment-selective sensitivity of cardiovascular morphogenesis to combinations of retinoic acid receptor gene mutations. Circ Res. 1997; 80:757–764. [PubMed: 9168777]

Li P, Pashmforoush M, Sucov HM. Retinoic acid regulates differentiation of the secondary heart field and TGFbeta-mediated outflow tract septation. Dev Cell. 2010; 18:480–485. [PubMed: 20230754]

Li X, Lufkin T. Cre recombinase expression in the floorplate, notochord and gut epithelium in transgenic embryos driven by the Hoxa-1 enhancer III. Genesis. 2000; 26:121–122. [PubMed: 10686604]

Lin SC, Dolle P, Ryckebusch L, Noseda M, Zaffran S, Schneider MD, Niederreither K. Endogenous retinoic acid regulates cardiac progenitor differentiation. Proc Natl Acad Sci U S A. 2010; 107:9234–9239. [PubMed: 20439714]

Lufkin T, Dierich A, LeMeur M, Mark M, Chambon P. Disruption of the Hox-1.6 homeobox gene results in defects in a region corresponding to its rostral domain of expression. Cell. 1991; 66:1105–1119. [PubMed: 1680563]

Ma Q, Zhou B, Pu WT. Reassessment of Isl1 and Nkx2-5 cardiac fate maps using a Gata4-based reporter of Cre activity. Dev Biol. 2008; 323:98–104. [PubMed: 18775691]

Macatee TL, Hammond BP, Arenkiel BR, Francis L, Frank DU, Moon AM. Ablation of specific expression domains reveals discrete functions of ectoderm- and endoderm-derived FGF8 during cardiovascular and pharyngeal development. Development. 2003; 130:6361–6374. [PubMed: 14623825]

Makki N, Capecchi MR. Hoxa1 lineage tracing indicates a direct role for Hoxa1 in the development of the inner ear, the heart, and the third rhombomere. Dev Biol. 2010; 341:499–509. [PubMed: 20171203]

Marshall H, Morrison A, Studer M, Popperl H, Krumlauf R. Retinoids and Hox genes. Faseb J. 1996; 10:969–978. [PubMed: 8801179]

Meilhac SM, Esner M, Kelly RG, Nicolas JF, Buckingham ME. The clonal origin of myocardial cells in different regions of the embryonic mouse heart. Dev Cell. 2004; 6:685–698. [PubMed: 15130493]

Merki E, Zamora M, Raya A, Kawakami Y, Wang J, Zhang X, Burch J, Kubalak SW, Kaliman P, Belmonte JC, Chien KR, Ruiz-Lozano P. Epicardial retinoid X receptor alpha is required for myocardial growth and coronary artery formation. Proc Natl Acad Sci U S A. 2005; 102:18455–18460. [PubMed: 16352730]

Mjaatvedt CH, Nakaoka T, Moreno-Rodriguez R, Norris RA, Kern MJ, Eisenberg CA, Turner D, Markwald RR. The outflow tract of the heart is recruited from a novel heart-forming field. Dev Biol. 2001; 238:97–109. [PubMed: 11783996]

Moss JB, Xavier-Neto J, Shapiro MD, Nayeem SM, McCaffery P, Drager UC, Rosenthal N. Dynamic patterns of retinoic acid synthesis and response in the developing mammalian heart. Dev Biol. 1998; 199:55–71. [PubMed: 9676192]

Murphy P, Hill RE. Expression of the mouse labial-like homeobox-containing genes, Hox 2.9 and Hox 1.6, during segmentation of the hindbrain. Development. 1991; 111:61–74. [PubMed: 1673098]

Niederreither K, Dolle P. Retinoic acid in development: towards an integrated view. Nat Rev Genet. 2008; 9:541–553. [PubMed: 18542081]

Niederreither K, Subbarayan V, Dolle P, Chambon P. Embryonic retinoic acid synthesis is essential for early mouse post-implantation development. Nat Genet. 1999; 21:444–448. [PubMed: 10192400]

Niederreither K, Vermot J, Messaddeq N, Schuhbaur B, Chambon P, Dolle P. Embryonic retinoic acid synthesis is essential for heart morphogenesis in the mouse. Development. 2001; 128:1019–1031. [PubMed: 11245568]

Rosenthal N, Xavier-Neto J. From the bottom of the heart: anteroposterior decisions in cardiac muscle differentiation. Curr Opin Cell Biol. 2000; 12:742–746. [PubMed: 11063942]

Rossant J, Zirngibl R, Cado D, Shago M, Giguere V. Expression of a retinoic acid response element-hsplacZ transgene defines specific domains of transcriptional activity during mouse embryogenesis. Genes Dev. 1991; 5:1333–1344. [PubMed: 1907940]

Rossel M, Capecchi MR. Mice mutant for both Hoxa1 and Hoxb1 show extensive remodeling of the hindbrain and defects in craniofacial development. Development. 1999; 126:5027–5040. [PubMed: 10529420]

Ryckebusch L, Wang Z, Bertrand N, Lin SC, Chi X, Schwartz R, Zaffran S, Niederreither K. Retinoic acid deficiency alters second heart field formation. Proc Natl Acad Sci U S A. 2008; 105:2913–2918. [PubMed: 18287057]

Searcy RD, Yutzey KE. Analysis of Hox gene expression during early avian heart development. Dev Dyn. 1998; 213:82–91. [PubMed: 9733103]

Sirbu IO, Gresh L, Barra J, Duester G. Shifting boundaries of retinoic acid activity control hindbrain segmental gene expression. Development. 2005; 132:2611–2622. [PubMed: 15872003]

Sirbu IO, Zhao X, Duester G. Retinoic acid controls heart anteroposterior patterning by down-regulating Isl1 through the Fgf8 pathway. Dev Dyn. 2008; 237:1627–1635. [PubMed: 18498088]

Soriano P. Generalized lacZ expression with the ROSA26 Cre reporter strain. Nat Genet. 1999; 21:70–71. [PubMed: 9916792]

Studer M, Gavalas A, Marshall H, Ariza-McNaughton L, Rijli FM, Chambon P, Krumlauf R. Genetic interactions between Hoxa1 and Hoxb1 reveal new roles in regulation of early hindbrain patterning. Development. 1998; 125:1025–1036. [PubMed: 9463349]

Studer M, Lumsden A, Ariza-McNaughton L, Bradley A, Krumlauf R. Altered segmental identity and abnormal migration of motor neurons in mice lacking Hoxb-1. Nature. 1996; 384:630–634. [PubMed: 8967950]

Theveniau-Ruissy M, Dandonneau M, Mesbah K, Ghez O, Mattei MG, Miquerol L, Kelly RG. The del22q11.2 candidate gene Tbx1 controls regional outflow tract identity and coronary artery patterning. Circ Res. 2008; 103:142–148. [PubMed: 18583714]

Tischfield MA, Bosley TM, Salih MA, Alorainy IA, Sener EC, Nester MJ, Oystreck DT, Chan WM, Andrews C, Erickson RP, Engle EC. Homozygous HOXA1 mutations disrupt human brainstem, inner ear, cardiovascular and cognitive development. Nat Genet. 2005; 37:1035–1037. [PubMed: 16155570]

Van Praagh, R. Semin Thorac Cardiovasc Surg Pediatr Card Surg Annu. 2009. The first Stella van Praagh memorial lecture: the history and anatomy of tetralogy of Fallot; p. 19-38.

Vincent SD, Buckingham ME. How to make a heart: the origin and regulation of cardiac progenitor cells. Curr Top Dev Biol. 2010; 90:1–41. [PubMed: 20691846]

Waldo KL, Kumiski DH, Wallis KT, Stadt HA, Hutson MR, Platt DH, Kirby ML. Conotruncal myocardium arises from a secondary heart field. Development. 2001; 128:3179–3188. [PubMed: 11688566]

Waxman JS, Keegan BR, Roberts RW, Poss KD, Yelon D. Hoxb5b acts downstream of retinoic acid signaling in the forelimb field to restrict heart field potential in zebrafish. Dev Cell. 2008; 15:923–934. [PubMed: 19081079]

Waxman JS, Yelon D. Increased Hox activity mimics the teratogenic effects of excess retinoic acid signaling. Dev Dyn. 2009; 238:1207–1213. [PubMed: 19384962]

Wellik DM. Hox genes and vertebrate axial pattern. Curr Top Dev Biol. 2009; 88:257–278. [PubMed: 19651308]

Xavier-Neto J, Neville CM, Shapiro MD, Houghton L, Wang GF, Nikovits W Jr, Stockdale FE, Rosenthal N. A retinoic acid-inducible transgenic marker of sino-atrial development in the mouse heart. Development. 1999; 126:2677–2687. [PubMed: 10331979]

Xavier-Neto J, Rosenthal N, Silva FA, Matos TG, Hochgreb T, Linhares VL. Retinoid signaling and cardiac anteroposterior segmentation. Genesis. 2001; 31:97–104. [PubMed: 11747199]

Yutzey KE, Rhee JT, Bader D. Expression of the atrial-specific myosin heavy chain AMHC1 and the establishment of anteroposterior polarity in the developing chicken heart. Development. 1994; 120:871–883. [PubMed: 7600964]

Zaffran S, Kelly RG, Meilhac SM, Buckingham ME, Brown NA. Right Ventricular Myocardium Derives From the Anterior Heart Field. Circ Res. 2004; 95:261–268. [PubMed: 15217909]

Zhang Z, Cerrato F, Xu H, Vitelli F, Morishima M, Vincentz J, Furuta Y, Ma L, Martin JF, Baldini A, Lindsay E. Tbx1 expression in pharyngeal epithelia is necessary for pharyngeal arch artery development. Development. 2005; 132:5307–5315. [PubMed: 16284121]

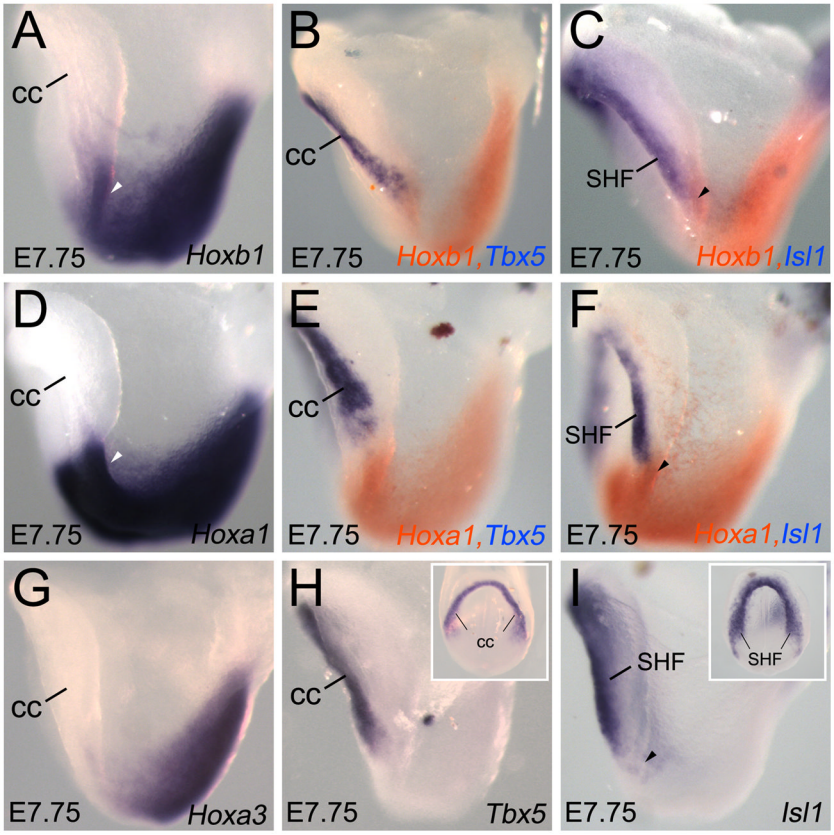

Figure 1.

Relation between *Hoxb1* and *Hoxa1* expression and the heart fields. (A–F) *Hoxb1* and *Hoxa1* expression analysis by single and double *in situ* hybridizations (ISH) on E7.75 embryos. (G) *Hoxa3* expression analysis by ISH. (H,I) Whole-mount ISH with *Tbx5* and *Islet1* (*Isl1*) probes, which mark the cardiac crescent (cc) and the second heart field (SHF) respectively. Insets display a ventral view of same stained embryo. (A,D,G) At E7.75, *Hoxb1*, *Hoxa1* and *Hoxa3* reach their most anterior border of expression near the cardiac crescent (cc). (B,C) Whole-mount ISH analysis showing that the anterior border of *Hoxb1* expression overlaps with *Isl1* (arrowhead in C), but not with *Tbx5*. (E,F) Whole-mount ISH analysis showing *Hoxa1* expression in an adjacent domain of *Tbx5* and *Isl1* (arrowhead in F). (G) Anterior border of *Hoxa3* expression is posterior to *Tbx5* and *Isl1* regions. cc, cardiac crescent; SHF, second heart field.

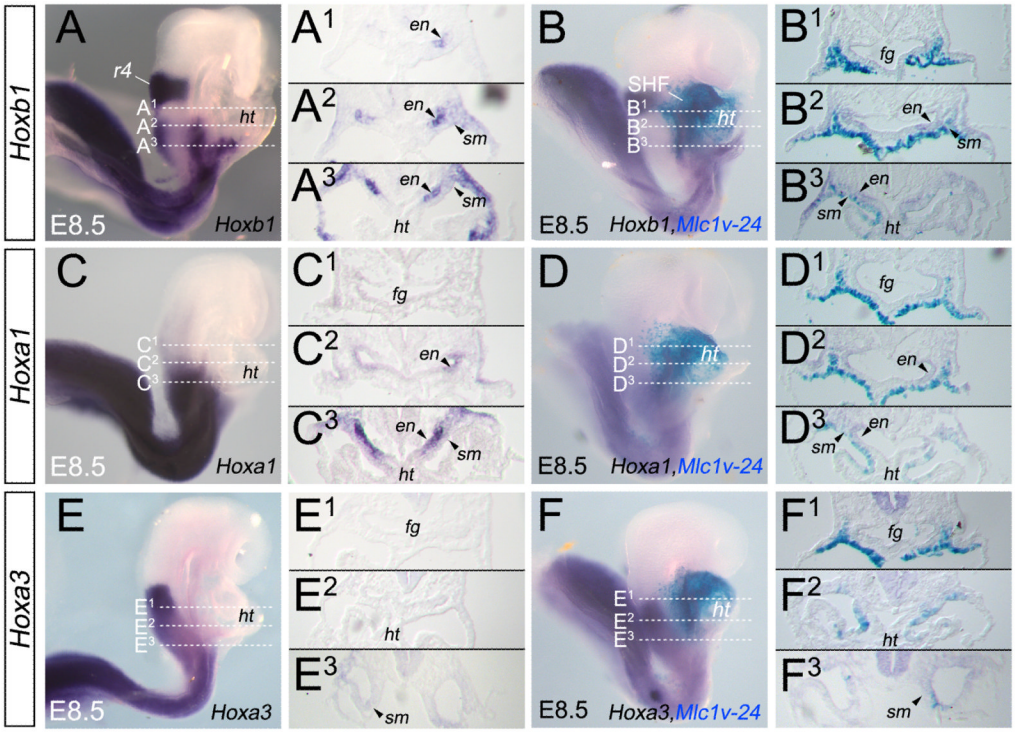

Figure 2.

Hoxb1 and *Hoxa1* expression patterns define distinct sub-domains within the second heart field. (A–F) Lateral views of embryos at E8.5. (A,C,E) Whole-mount *in situ* hybridization (ISH) analysis of *Hoxb1* (A), *Hoxa1* (C) and *Hoxa3* (E) mRNAs. (B,D,F) Whole-mount ISH analysis of *Hoxb1* (B), *Hoxa1* (D) and *Hoxa3* (F) genes combined with X-gal staining for the *Mlc1v-nlacZ-24* transgene, which marks the anterior heart field (AHF). Dotted lines in A–F indicate the plane of sections in A1–F2. (A1–A3) Sections showing expression of *Hoxb1* in the medial (A2, arrowhead) and posterior (A3) domains of the second heart field (SHF), and the absence of expression in the anterior domain of the SHF (A1). Note the expression of *Hoxb1* in the anterior foregut endoderm. (B1–B3) Sections showing co-localization of *Hoxb1* and X-gal staining in the caudal region of the AHF (B2,B3) but not in the anterior region of the AHF (B1). (C1–C3) Expression of *Hoxa1* is only detected in the posterior region of the SHF (C3, arrowheads). Note the expression of *Hoxa1* in the anterior foregut endoderm (C2, C1). (D1–D3) Sections showing the co-localization of *Hoxa1* and X-gal labeled cells only in the posterior region of the AHF (D3, arrowhead). (E1–E3) *Hoxa3* expression is observed in the splanchnic mesoderm (E3, arrowhead) located posteriorly to the heart tube. (F1–F3) Sections showing that *Hoxa3* is not detected in the AHF. cc, cardiac crescent; en, endoderm; fg, foregut; ht, heart tube; SHF, second heart field; sm, splanchnic mesoderm.

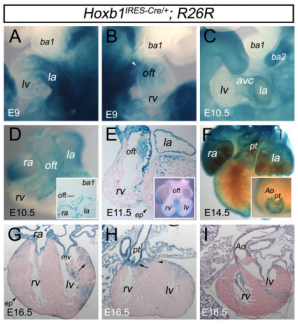

Figure 3.

Genetic lineage analysis reveals a contribution of *Hoxb1*$^{+}$ cardiac progenitors to the atria and the myocardium at the base of the pulmonary trunk. (A–I) *Hoxb1*-lineage visualized by X-gal staining of *Hoxb1*$^{IRES\text{-}Cre}$*; R26R-lacZ* embryos. (A–C) Lateral views of X-gal stained embryos at E9 (A,B) and E10.5 (C). (D–F) Ventral views of X-gal stained hearts at E10.5 (D), E11.5 (E) and E14.5 (F). (G,I) Transverse sections of X-gal stained hearts at E16.5. (A,B) X-gal staining showing a contribution of *Hoxb1*-positive cells to the venous pole (left atrium) and arterial pole (white arrowhead) of *Hoxb1*$^{IRES\text{-}Cre}$; *R26R-lacZ* hearts. (C) Lateral view of an E10.5 X-gal stained embryo, showing β-galactosidase activity in the left atrium and the atrioventricular canal. Note that neural crest derivatives populate the second branchial arch (ba2). (D) Ventral view of X-gal stained heart from *Hoxb1*$^{IRES\text{-}Cre}$*; R26R-lacZ* embryo at E10.5. β-galactosidase activity is detected in the left and right atria but also in the outflow tract (OFT). Inset is a frontal section through stage E10.5 embryo, showing β-galactosidase activity only in the inferior wall of the OFT. (E) Transverse section of the heart from an E11.5 *Hoxb1*$^{IRES\text{-}Cre}$*; R26R-lacZ* embryo. β-galactosidase activity is detected in the atria, the epicardium (arrowhead) and the left side of the OFT. Inset shows a ventral view of the same X-gal stained heart. (F) Ventral view of an X-gal stained heart at E14.5, showing that labeled cells are detected in right and left atria and at the base of the pulmonary trunk. Inset is a cranial view of the same heart. X-gal stained cells are concentrated at the base of the pulmonary trunk. (G–I) Transverse sections of an E16.5 heart. β-galactosidase activity is detected in the epicardium (arrowhead), the atrioventricular valves and in the myocardium at the base of the pulmonary trunk (arrow in H) but not at the base of the aorta (I). Arrow in G indicates X-gal stained cells in the left ventricular myocardium. Ao, aorta; avc, atrioventricular canal; ba, branchial arch; ep, epicardium; ht, heart tube; la, left atrium; lb, limb bud; lv, left ventricle; mv; mitral valve; oft, outflow tract; pt, pulmonary trunk; ra, right atrium; rv; right ventricle.

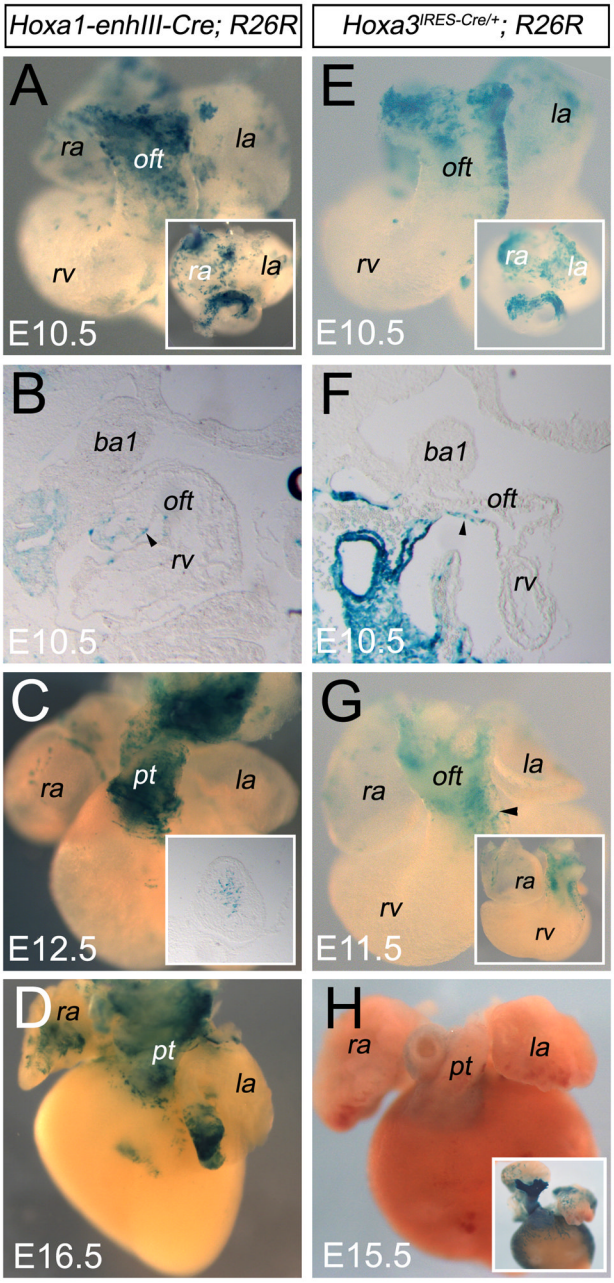

Figure 4.

Cardiac contribution of the *Hoxa1-enhIII-Cre and Hoxa3*$^{IRES\text{-}Cre}$ progeny. (A–D) *Hoxa1*-lineage visualized by X-gal staining of *Hoxa1-enhIII-Cre; R26R-lacZ* embryos. (E–H) *Hoxa3*-lineage visualized by X-gal staining of *Hoxa3*$^{IRES\text{-}Cre}$*; R26R-lacZ* embryos. Ventral views of X-gal stained hearts at E10.5 (A,E), E11.5 (G), E12.5 (C), E15.5 (H) and E16.5 (D). (A,E) β-galactosidase activity is detected in small number of left and right atrial cells. X-gal staining is observed in the distal outflow tract (OFT) in *Hoxa1-enhIII-Cre; R26R-lacZ* and *Hoxa3*$^{IRES\text{-}Cre}$*; R26R-lacZ* embryos. Insets show cranial views of the same hearts confirming β-galactosidase activity in the inferior wall of the OFT. (B,F) Sagittal sections of embryos at the same stage showing X-gal labeled cells in the inferior wall of the OFT. (C,D) Ventral views of X-gal stained hearts at E12.5 and E16.5. β-galactosidase activity is

detected in both atria and in the myocardium at the base of the pulmonary trunk. Inset in C displays X-gal labeled cells in the OFT cushions. (G,H) Ventral views of X-gal stained hearts at E11.5 and E15.5, showing that few labeled cells are detected in the left side of the OFT (arrowhead) and later in the myocardium at the base of the pulmonary trunk. Inset in G reveals X-gal labeled cells in OFT cushions. Inset in H shows a ventral view of stronger X-gal stained heart at the same stage. Ao, aorta; b, branchial arch; g, gut epithelium; ht, heart tube; la, left atrium; lb, limb bud; oft, outflow tract; pt, pulmonary trunk; ra, right atrium; rv; right ventricle.

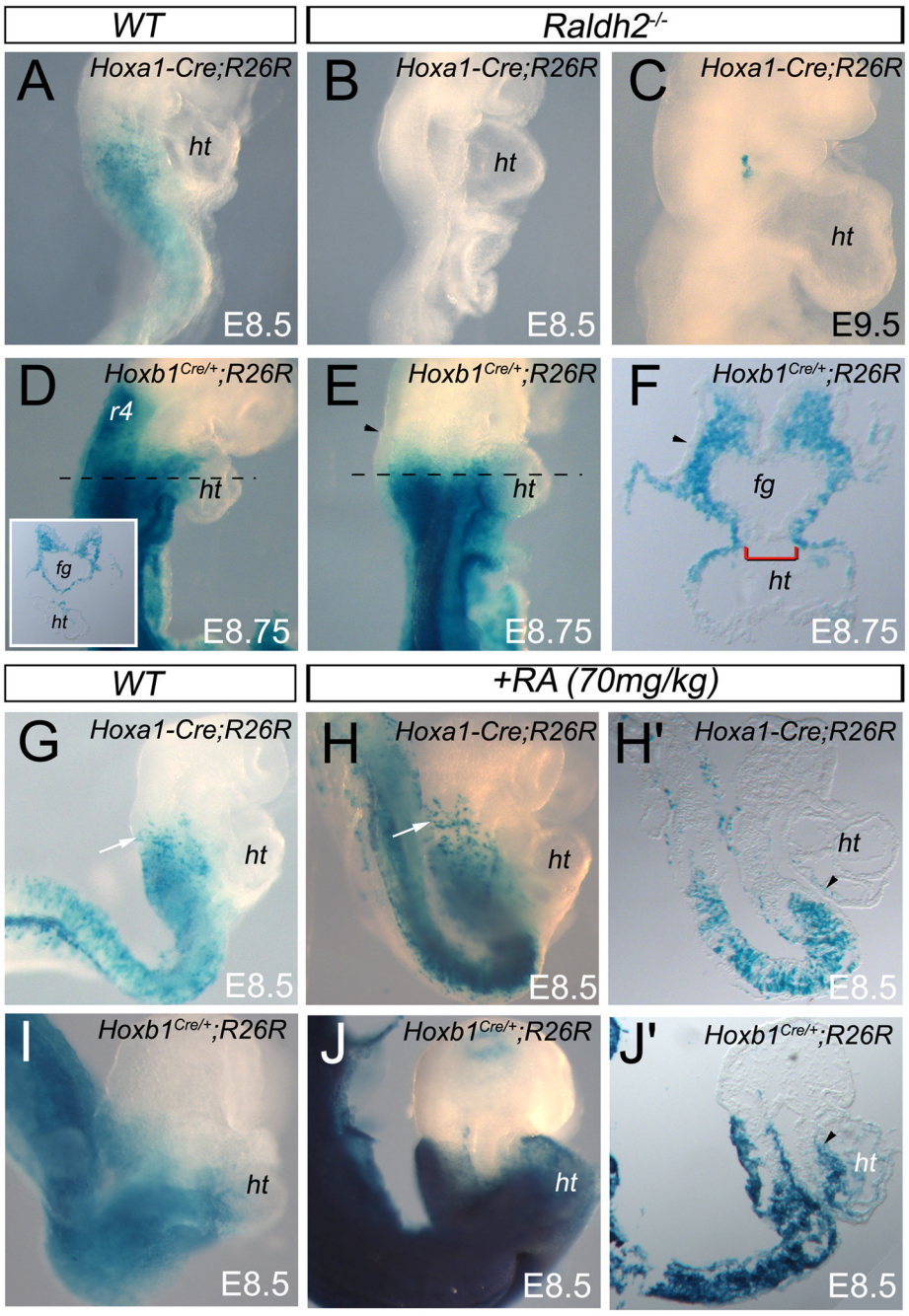

Figure 5.

Reduction or excess of RA signaling causes abnormalities of *Hoxa1*$^{+}$ and *Hoxb1*$^{+}$ cardiac progenitors contribution. (A–J) Lateral views of E8.5 (A,B,G–J), E8.75 (D–F) and E9.5 (C) embryos. (A–C) β-galactosidase activity is detected in *Hoxa1-enhIII-Cre; R26R* embryo, whereas no X-gal labeled cells are observed in *Hoxa1-enhIII-Cre; R26R; Raldh2*$^{-/-}$ mutant embryos, which reveals the requirement of retinoic acid (RA) for the induction of this transgene. (D,E) Lateral view of X-gal stained *Hoxb1*$^{IRES\text{-}Cre}$*; R26R-lacZ* embryos at E8.75. (F) Transverse section of the embryo shown in E at the heart tube level. Inset in D shows a similar transverse section in the control embryo. X-gal labeled cells are yet detected in *Raldh2*$^{-/-}$ (E,F) mutant embryo. (F) Sections confirm that dorsal mesocardium is not closed

in mutant embryos (brackets). Note the absence of X-gal staining in the surface ectoderm (arrowhead), suggesting differential response to deficiency in RA signaling. (G,H) X-gal staining showing intensify activity of *Hoxa1-enhIII-Cre* transgene (arrows) in the anterior domain of RA-treated embryos. (H′) Sagittal section of the embryo in H showing X-gal labeled cells in the heart tube (arrowhead). (I,J) X-gal staining showing increase of *Hoxb1*$^{\text{IRES-Cre}}$ in *Hoxb1*$^{IRES\text{-}Cre}$; *R26R-lacZ* embryos treated with all-*trans*-RA. (J′) Sagittal section exhibits β-galactosidase activity in the heart tube (arrowhead) of the embryo shown in J. ht, heart tube.

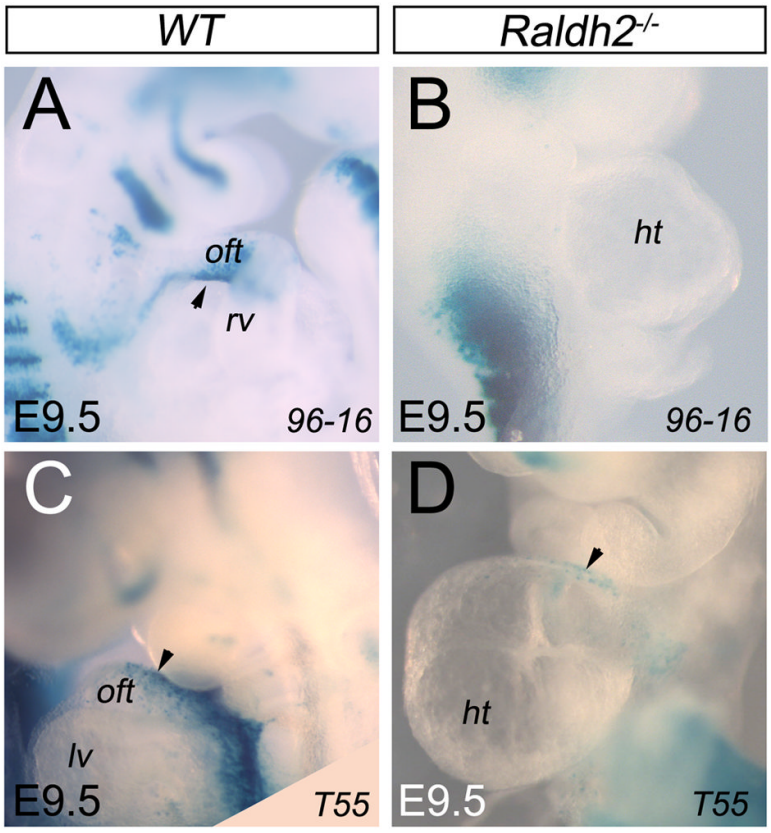

Figure 6.

Reduction of RA signaling induces defect of the inferior wall of the outflow tract. (A,B) X-gal staining showing absence of *y96-Myf5-nlacZ-16* (*96-16*) transgene expression in *Raldh2*$^{-/-}$ (B) embryos at E9.5. (C,D) At E9.5, β-galactosidase activity is detected in the superior wall of the heart tube of *A17-Myf5-nlacZ-T55* (*T55*); *Raldh2*$^{-/-}$ (D) embryos. ht, heart tube; lv, left ventricle; oft, outflow tract; rv, right ventricle.

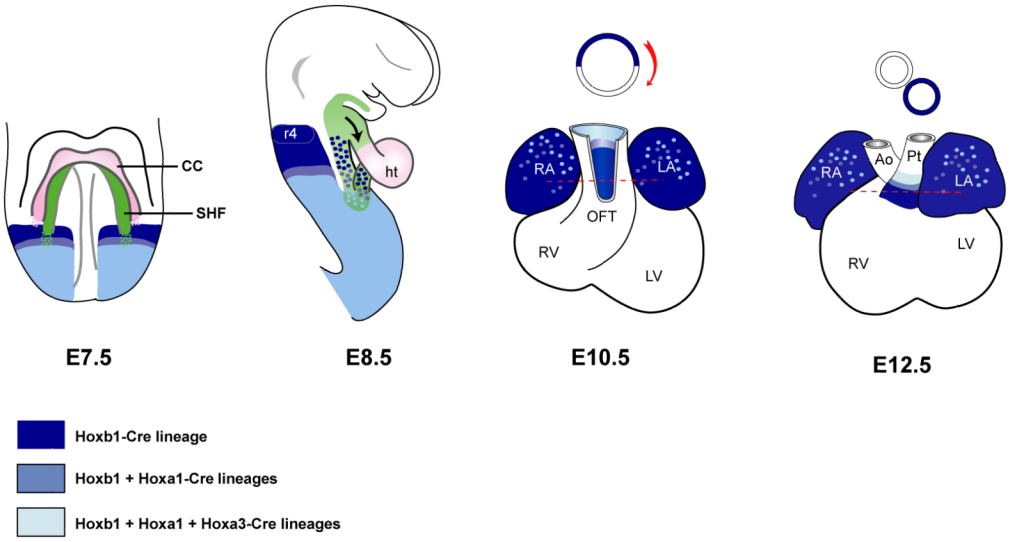

Figure 7.

Model for cardiac contributions of progenitor cells expressing *Hox* genes in the second heart field. Genetic lineage analysis was made with *Hoxb1*^{Cre}, *Hoxa1-EnhIII-Cre*, *Hoxa3*^{Cre} and R26R-lacZ lines. X-gal stained cells are represented by blue colors. The location of the second heart field (SHF) is shown in green. Frontal view is shown for embryonic day 7.5 (E7.5) and lateral view for E8.5. Early *Hoxb1/a1/a3* expressing cells characterize distinct subdomains along the antero-posterior axis in the SHF. Later, these cardiac progenitor cells contribute to both atria and the inferior wall of the OFT, which subsequently gives rise to myocardium at the base of pulmonary trunk. Ao, aorta; CC, cardiac crescent; ep, epicardium; ht, heart tube; LA, left atria; Pt, pulmonary trunk; RA, right atria, r4, rhombomere 4.